

# $\mu$ O-conotoxin MrVIB selectively blocks $\text{Na}_v1.8$ sensory neuron specific sodium channels and chronic pain behavior without motor deficits

J. Ekberg\*<sup>†</sup>, A. Jayamanne<sup>‡</sup>, C. W. Vaughan<sup>‡</sup>, S. Aslan<sup>‡</sup>, L. Thomas<sup>\*</sup>, J. Mould\*<sup>†</sup>, R. Drinkwater\*<sup>§</sup>, M. D. Baker<sup>¶</sup>, B. Abrahamsen<sup>¶</sup>, J. N. Wood<sup>¶</sup>, D. J. Adams<sup>†</sup>, M. J. Christie\*<sup>¶</sup>, and R. J. Lewis\*<sup>¶</sup>

\*Institute for Molecular Bioscience and <sup>†</sup>School of Biomedical Sciences, University of Queensland, QLD 4072, Australia; <sup>‡</sup>Pain Management Research Institute and Kolling Institute, Northern Clinical School, University of Sydney at Royal North Shore Hospital, St Leonards, NSW 2065, Australia; and <sup>¶</sup>Molecular Nociception Group, Department of Biology, University College of London, Gower Street, London WC1E 6BT, United Kingdom

Edited by William A. Catterall, University of Washington School of Medicine, Seattle, WA, and approved September 1, 2006 (received for review March 6, 2006)

**The tetrodotoxin-resistant voltage-gated sodium channel (VGSC)  $\text{Na}_v1.8$  is expressed predominantly by damage-sensing primary afferent nerves and is important for the development and maintenance of persistent pain states. Here we demonstrate that  $\mu$ O-conotoxin MrVIB from *Conus marmoreus* displays substantial selectivity for  $\text{Na}_v1.8$  and inhibits pain behavior in models of persistent pain. In rat sensory neurons, submicromolar concentrations of MrVIB blocked tetrodotoxin-resistant current characteristic of  $\text{Na}_v1.8$  but not  $\text{Na}_v1.9$  or tetrodotoxin-sensitive VGSC currents. MrVIB blocked human  $\text{Na}_v1.8$  expressed in *Xenopus* oocytes with selectivity at least 10-fold greater than other VGSCs. In neuropathic and chronic inflammatory pain models, allodynia and hyperalgesia were both reduced by intrathecal infusion of MrVIB (0.03–3 nmol), whereas motor side effects occurred only at 30-fold higher doses. In contrast, the nonselective VGSC blocker lignocaine displayed no selectivity for allodynia and hyperalgesia versus motor side effects. The actions of MrVIB reveal that VGSC antagonists displaying selectivity toward  $\text{Na}_v1.8$  can alleviate chronic pain behavior with a greater therapeutic index than nonselective antagonists.**

electrophysiology | pain model | dorsal root ganglia | allodynia |  $\delta$ -conotoxin

Voltage-gated sodium channels (VGSCs) are an established target for a number of classes of analgesic drugs, including local anesthetics and antiepileptics (1). Unfortunately, VGSC inhibitors show limited selectivity for pain versus other sensory and motor neurotransmission pathways in the periphery, despite possessing functional selectivity associated with activity-dependent block (1). Among the VGSC  $\alpha$ -subunit subtypes known to mediate action potential generation in mammals,  $\text{Na}_v1.8$  is a particularly promising candidate for development of subtype-selective VGSC therapeutics for persistent pain (1, 2). VGSC subtypes exhibit differential tissue distribution, but only  $\text{Na}_v1.8$  is expressed exclusively by primary afferent neurons (3, 4). Functional characterization has revealed that >85% of neurons expressing  $\text{Na}_v1.8$  are nociceptors (5). The kinetic properties and distribution of  $\text{Na}_v1.8$  within nociceptive sensory neurons also indicate that it is associated with the pathology that develops in persistent pain states (5, 6).  $\text{Na}_v1.8$  is redistributed into peripheral regions of sensory nerves after injury in animal models (7, 8) and humans (9, 10), and the behavioral changes in response to pain after antisense knockdown have suggested an important role in neuropathic pain (7, 11).  $\text{Na}_v1.8$  knockout mice have established that this channel is involved in the generation of aberrant activity in neuromas (12) and is essential for normal noxious mechanosensation (4). Furthermore,  $\text{Na}_v1.8$  plays an important role in the development of inflammatory hyperalgesia (3, 4).

In this study we searched for selective  $\text{Na}_v1.8$  inhibitors among the rich diversity of conotoxins found in the venoms of fish-

mollusk-, and worm-hunting cone snails (13). After screening crude venoms from  $\approx 30$  species, we identified two closely related conotoxins,  $\mu$ O-conotoxin MrVIA and  $\mu$ O-conotoxin MrVIB (MrVIB), which selectively inhibited the tetrodotoxin-resistant (TTX-R) sodium current without affecting calcium current in sensory neurons (14). Here, we determine the VGSC subtype-selectivity of MrVIB in rat sensory neurons and heterologous expression systems and establish its selectivity for pain pathways in rat models of persistent pain.

## Results and Discussion

We first assessed the selectivity of MrVIB to block VGSC currents in rat dorsal root ganglion (DRG) neurons. In nociceptive DRG neurons, tetrodotoxin-sensitive (TTX-S) currents are carried by  $\text{Na}_v1.1$ , -1.2, -1.6, and -1.7 subtypes, with a minor contribution from  $\text{Na}_v1.3$  (2). In the presence of TTX and when recording conditions that inactivate  $\text{Na}_v1.9$  but not  $\text{Na}_v1.8$  were used, MrVIB was >10-fold more potent at blocking TTX-R currents than TTX-S  $\text{Na}^+$  currents (Fig. 1A). Inhibition by MrVIB lacked voltage-dependence, in contrast to  $\delta$ -conotoxins, which can have voltage-dependent effects (15). The  $\text{IC}_{50}$  for inhibition of TTX-R by MrVIB was 98 nM [95% confidence interval (C.I.), 86–113 nM;  $n = 6$ ] versus 1.1  $\mu\text{M}$  (95% C.I., 0.93–1.3  $\mu\text{M}$ ;  $n = 6$ ) for the TTX-S  $\text{Na}^+$  current under these conditions. Conversely, when TTX (300 nM) and recording conditions to enhance currents through  $\text{Na}_v1.9$  by removing ultra-slow inactivation (16) were used, MrVIB at concentrations up to 10  $\mu\text{M}$  had no effect on this persistent TTX-R  $\text{Na}^+$  current, indicating that MrVIB inhibits  $\text{Na}_v1.8$  >100-fold more potently than it inhibits  $\text{Na}_v1.9$ .

We next examined whether MrVIB was selective for individual VGSC subtypes expressed heterologously in *Xenopus* oocytes. Consistent with the result obtained in rat DRG neurons, MrVIB inhibited human (h) $\text{Na}_v1.8$  with an  $\text{IC}_{50}$  of 102 nM (95% C.I.,

Author contributions: J.E. and A.J. contributed equally to this work; J.E., C.W.V., R.D., M.D.B., J.N.W., D.J.A., M.J.C., and R.J.L. designed research; J.E., A.J., S.A., L.T., J.M., R.D., M.D.B., and B.A. performed research; L.T., R.D., and R.J.L. contributed new reagents/analytic tools; J.E., A.J., S.A., J.M., B.A., J.N.W., D.J.A., M.J.C., and R.J.L. analyzed data; and J.E., A.J., C.W.V., M.D.B., J.N.W., D.J.A., M.J.C., and R.J.L. wrote the paper.

The authors declare no conflict of interest.

This article is a PNAS direct submission.

Freely available online through the PNAS open access option.

Abbreviations: CFA, complete Freund's adjuvant; C.I., confidence interval; DRG, dorsal root ganglion; PNL, partial ligation of the sciatic nerve; PWL, paw withdrawal latency; PWT, paw withdrawal threshold; TTX-R, tetrodotoxin-resistant; TTX-S, tetrodotoxin-sensitive; VGSC, voltage-gated sodium channel.

<sup>§</sup>Present address: Xenome Ltd., 120 Meiers Road, Indooroopilly, QLD 4068, Australia.

<sup>¶</sup>To whom correspondence may be addressed. E-mail: macc@med.usyd.edu.au or r.lewis@imb.uq.edu.au.

© 2006 by The National Academy of Sciences of the USA

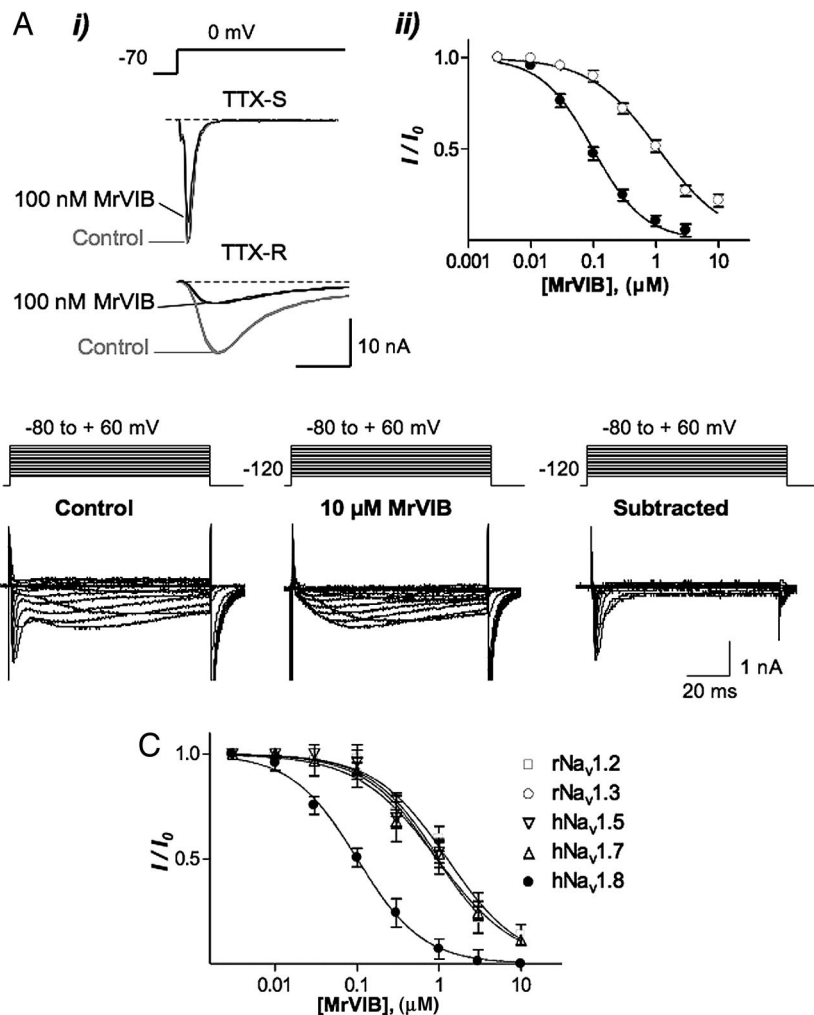


**Fig. 1.** MrVIB selectively blocks a TTX-R current in DRG and Na<sub>v</sub>1.8. (A) Inhibition of transient TTX-S and TTX-R Na<sup>+</sup> currents in rat DRG neurons by MrVIB. (A*i*) Superimposed depolarization-activated TTX-S and TTX-R Na<sup>+</sup> currents in the absence (control) and presence of 100 nM MrVIB. The TTX-S Na<sup>+</sup> current was recorded from a large ( $\approx 45\text{-}\mu\text{m}$ -diameter) DRG neuron that exhibited a Na<sup>+</sup> current with fast activation and inactivation kinetics that was 95% inhibited by 300 nM TTX, whereas the TTX-R Na<sup>+</sup> current was recorded from a small ( $\leq 25\text{-}\mu\text{m}$ -diameter) neuron in the presence of 300 nM TTX. (A*ii*) Comparison of toxin inhibition of TTX-R (●) versus TTX-S (○) Na<sup>+</sup> current. The half-maximal inhibitory concentration ( $IC_{50}$ ) was 98 nM ( $n = 6$ ) for the TTX-R Na<sup>+</sup> current and 1.1  $\mu\text{M}$  ( $n = 6$ ) for the TTX-S Na<sup>+</sup> current. (B) MrVIB has no effect on the persistent TTX-R Na<sup>+</sup> current in rat DRG neurons. Currents obtained from a DRG neuron containing both slowly inactivating (Na<sub>v</sub>1.8) and persistent (Na<sub>v</sub>1.9) TTX-R Na<sup>+</sup> currents in the absence (control) and presence of 10  $\mu\text{M}$  MrVIB. TTX (300 nM) were present throughout the experiment. Neurons were held at  $-120$  mV and depolarized to voltages ranging from  $-80$  to  $+60$  mV in 10-mV increments, generating slowly inactivating and persistent Na<sup>+</sup> currents of different amplitude. MrVIB at 10  $\mu\text{M}$  completely inhibited the slowly inactivating TTX-R Na<sup>+</sup> current, although leaving the persistent TTX-R Na<sup>+</sup> current intact. Subtraction of the Na<sup>+</sup> currents recorded in presence of MrVIB from control Na<sup>+</sup> current resulted in typical Na<sub>v</sub>1.8 currents, further demonstrating that MrVIB at 10  $\mu\text{M}$  completely inhibits Na<sub>v</sub>1.8 but not Na<sub>v</sub>1.9. (C) Concentration–response relationship for MrVIB inhibition of different VGSC subtypes expressed in *Xenopus* oocytes. The  $IC_{50}$  for MrVIB was 102 nM for human (h)Na<sub>v</sub>1.8 and  $\approx 1$   $\mu\text{M}$  for rat (r)Na<sub>v</sub>1.2, rNa<sub>v</sub>1.3, hNa<sub>v</sub>1.5, and hNa<sub>v</sub>1.7 ( $n = 3\text{--}6$ ).  $I$  represents the maximal Na<sup>+</sup> current amplitude recorded in the presence of MrVIB at various concentrations, and  $I_0$  represents the maximal Na<sup>+</sup> current obtained in the absence of toxin. Only oocytes that expressed VGSC currents  $>200$  nA were used in this study. For comparison, MrVIB has been shown to inhibit the muscle-type VGSC Na<sub>v</sub>1.4 with an  $IC_{50}$  value of 222 nM (MrVIA showed a comparable potency of 265 nM) (17).

82–126 nM;  $n = 6$ ), whereas at rat (r)Na<sub>v</sub>1.2, rNa<sub>v</sub>1.3, hNa<sub>v</sub>1.5, and hNa<sub>v</sub>1.7, MrVIB inhibited current with an  $IC_{50}$  of  $\approx 1$   $\mu\text{M}$  ( $n = 3\text{--}6$  at each subtype) (Fig. 1C). Together with results from rat DRG neurons, these data establish MrVIB as a potent inhibitor of rat and human Na<sub>v</sub>1.8, with  $\approx 10$ -fold lower potency for sensory neuron specific Na<sub>v</sub>1.1, 1.6, and 1.7, and  $>100$ -fold lower potency to inhibit Na<sub>v</sub>1.9. MrVIB has been reported to also inhibit the skeletal muscle VGSC subtype Na<sub>v</sub>1.4 ( $IC_{50}$  of 222 nM) (17), suggesting that MrVIB has a preference for Na<sub>v</sub>1.8 and Na<sub>v</sub>1.4 over other VGSC subtypes.

We then determined the ability of intrathecal infusions of MrVIB to reverse neuropathic and inflammatory pain established in rats. Fourteen days after surgery, MrVIB reduced neuropathic pain behavior in a nerve injury model of persistent

pain at doses below those causing motor side effects as assessed by rotarod latency. Partial ligation of the sciatic nerve (PNL) reduced both mechanical paw withdrawal threshold (PWT) and thermal paw withdrawal latency (PWL) (Fig. 2A and C). In these animals, intrathecal injection of MrVIB (0.01–3.0 nmol) produced a dose-dependent increase in mechanical PWT and thermal PWL that reached a maximum at 1–2 h after injection and declined within 4–6 h (Fig. 2A and C;  $n = 5\text{--}11$ ). MrVIB increased mechanical PWT in biphasic dose ranges ( $ED_{50} = 0.02 \pm 0.01$  and  $0.67 \pm 0.35$  nmol), thermal PWL in a single monophasic dose range ( $ED_{50} = 0.38 \pm 0.50$  nmol), and at much higher doses decreased rotarod latency ( $ED_{50} > 3$  nmol; Fig. 3A). Injection of vehicle alone produced no significant change in mechanical PWT, thermal PWL, or rotarod latency (Fig. 2A–D;

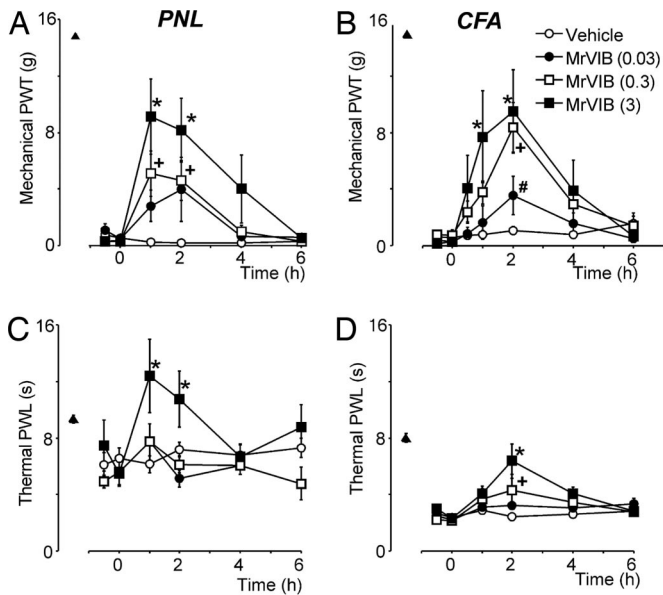


**Fig. 2.** MrVIB reduces allodynic and hyperalgesic behavior in neuropathic and inflammatory pain models. Shown are time plots of the effect of MrVIB (for clarity only 0.03, 0.3, and 3.0 nmol doses are shown; ●, □, and ■, respectively), or vehicle (○) on mechanical paw withdrawal threshold (PWT) (A and B). Thermal paw withdrawal latency (PWL) (C and D) in animals that had undergone partial ligation of the sciatic nerve (PNL) 14 days before the experiment (A and C), or complete Freund's adjuvant (CFA) injection into the plantar surface of the hindpaw 24 h before the experiment (B and D). The pre-PNL and pre-CFA mechanical PWT and thermal PWL are also shown (▲). Data are shown as the mean ± SEM. \* and + denote  $P < 0.05$  for 0.3 and 3 nmol compared with time 0, respectively.

Fig. 3 A–D;  $P > 0.05$ ,  $n = 6–8$ ). The lowest dose of MrVIB producing significant inhibition of mechanical allodynia [0.1 nmol both for 2 h after injection (data not shown) and integrated time-response data (Fig. 3A)] was >30-fold less than the dose producing significant motor side effects, indicating that MrVIB may inhibit signs of neuropathic pain behavior by a selective action on  $Na_v1.8$ . Although higher doses were needed to maximally inhibit mechanical allodynia and thermal hyperalgesia (Fig. 3A), these TTX-R currents were still at least 10-fold less than doses producing motor deficits. No other behavioral side effects, such as the ataxia produced by local anesthetics or the shaking produced by  $\omega$ -conotoxins (18), were observed at the highest doses of MrVIB tested. By contrast, intrathecal lignocaine lacked selectivity for mechanical PWT and thermal PWL versus rotarod latency, with  $ED_{50}$ s of  $0.12 \pm 0.10$ ,  $0.2 \pm 0.14$ , and  $0.20 \pm 0.40$  mg, respectively (Fig. 3C).

MrVIB also produced selective inhibition of sensory signs of pain behavior in an inflammatory pain model. Intraplantar CFA injection reduced both mechanical PWT and thermal PWL after 24 h (Fig. 2B and D). As in the neuropathic model, MrVIB produced an increase in mechanical PWT and thermal PWL, which reached a maximum at 2 h after injection and declined within 4–6 h (Fig. 2B and D,  $n = 5–8$ ). The lowest dose of MrVIB producing significant effects on mechanical PWT 2 h after injection was 0.03 nmol (Fig. 2B). No effects were observed on mechanical or thermal withdrawal latencies in the uninflamed paw (data not shown). The increases in mechanical PWT ( $ED_{50} = 0.02 \pm 0.01$  and  $2.8 \pm 2.5$  nmol), thermal PWL (lowest dose for significant effect at 2 h after injection was 0.3 nmol,  $ED_{50} > 3$  nmol), and the decrease in rotarod latency (significant effect only at 3.0 nmol at 2 h after injection,  $ED_{50} > 3$  nmol) were dose-dependent (Fig. 3B), again demonstrating a 10- to 30-fold selectivity for signs of mechanical pain behavior versus motor

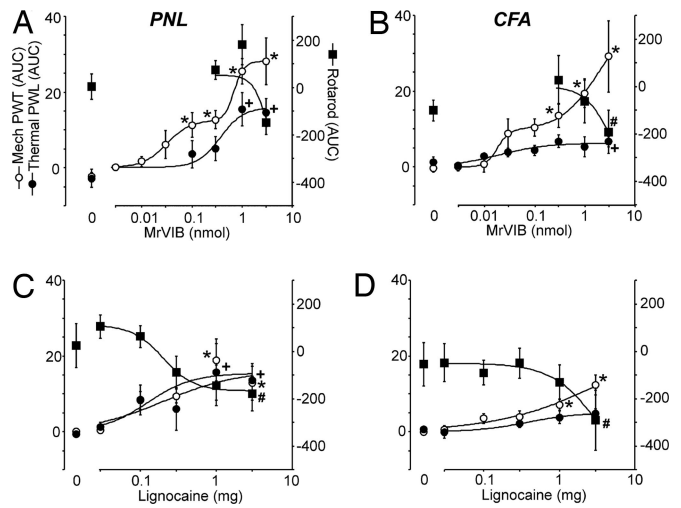


**Fig. 3.** MrVIB reduces allodynia and hyperalgesia at doses below those producing motor disruption. Dose–response curves were determined from area under time–response curves [AUC calculated by using the preinjection response (–0.5 h) as shown in Fig. 2 as a baseline for integration; same scales for A–D]. The effects of MrVIB (A and B) and lignocaine (C and D) on mechanical PWT (○), thermal PWL (●), and rotarod latency (■) in animals that had undergone PNL (A and C) or CFA injection (B and D). Logistic functions were fit to determine  $ED_{50}$ s. Data are shown as the mean ± SEM. \*, +, and # denote  $P < 0.05$  for mechanical PWT, thermal PWL, and rotarod latency compared with control, respectively. AUCs for PWT, PWL, and rotarod responses to saline are shown to the left of the abscissa.

deficits. Injection of vehicle alone produced no significant change in mechanical PWT, thermal PWL, or rotarod latency (Fig. 3A and D;  $P > 0.05$ ,  $n = 6–8$ ). As in the neuropathic model, intrathecal lignocaine lacked selectivity for mechanical PWT and thermal PWL versus rotarod latency, with  $ED_{50}$ s of  $4.3 \pm 1.7$ ,  $0.38 \pm 0.11$ , and  $1.3 \pm 0.3$  mg, respectively (Fig. 3D).

MrVIB also displayed antinociceptive activity after localized peripheral injection. Intraplantar injection of MrVIB reduced the second, but not the first, phase nociceptive response produced by intraplantar formalin (Fig. 4 and *Inset*). This finding suggests that peripheral application of MrVIB blunts sensitized nociceptive responses, without affecting the acute phase medi-

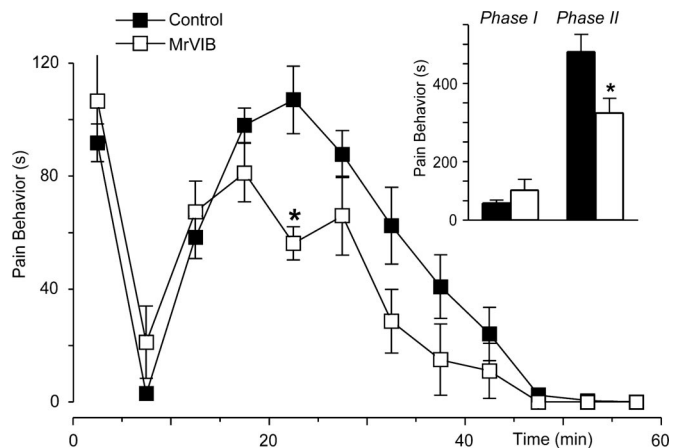


**Fig. 4.** Effects of MrVIB on phase I and phase II formalin responses. Influence of s.c. MrVIB vs. saline (control) on the time course of pain behaviors (biting, licking) 5 min subsequent to ipsilateral formalin injection (30) is shown. (*Inset*) Cumulative responses for control (solid bars) and MrVIB (open bars) treatments for phase I (0–10 min) and phase II (15–45 min) of the response. Error bars = SEM, and \*,  $P < 0.05$ .



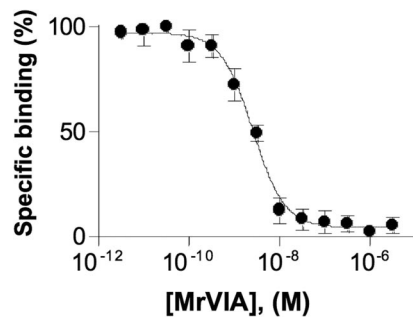


**Fig. 5.** MrVIA displaced binding of  $^{125}\text{I}$ -TxVIA to rat brain membranes. Concentration response for MrVIA displacement of  $^{125}\text{I}$ -TxVIA binding to rat brain membranes ( $\text{IC}_{50} = 2.8 \text{ nM}$ ; 95% C.I., range 2.1–3.7 nM,  $n = 3$ ). Nonspecific binding of  $^{125}\text{I}$ -TxVIA was determined in the presence of a saturating concentration of unlabeled TxVIA ( $10 \mu\text{M}$ ) and subtracted from all values.

ated by direct sensory stimulation (first phase). In other experiments, intraplantar injection of MrVIB did not affect nociceptive responses to intraplantar carrageenan, prostaglandin (PG), or nerve growth factor (NGF) (data not shown). Recent data suggest that  $\text{Na}_v1.7$  plays a dominant role in the response to these inflammatory mediators (19). Again, although antisense oligonucleotides directed against  $\text{Na}_v1.8$  partially blocked  $\text{PGE}_2$ -induced thermal hyperalgesia, the  $\text{Na}_v1.8$  knockout showed a normal hyperalgesic response to  $\text{PGE}_2$  (20, 21). NGF acts indirectly on  $\text{Na}_v1.8$  expression, possibly via p11 (22), as well as through second messengers (23), and also on a variety of receptors implicated in inflammatory hyperalgesia, including TRPV1 (24). Thus the lack of effect of MrVIB in these models is consistent with most published data.

The  $\mu\text{O}$ -conotoxins are structurally related to  $\delta$ -conotoxins, but the latter delay VGSC inactivation rather than blocking the current (25) producing enhancement of VGSC activity. Surprisingly, we found that  $\mu\text{O}$ -conotoxin (MrVIA) was a potent inhibitor of  $^{125}\text{I}$ -labeled  $\delta$ -conotoxin ( $^{125}\text{I}$ -TxVIA) binding to VGSCs (Fig. 5;  $\text{IC}_{50} = 2.8 \text{ nM}$ ), indicating that the  $\mu\text{O}$ - and  $\delta$ -conotoxins share an overlapping binding site on the VGSC. It appears that toxins acting at this site can either act to inhibit VGSC ion conduction (MrVIA and MrVIB) or delay inactivation ( $\delta$ -conotoxins). The  $\delta$ -conotoxin binding site includes the hydrophobic triad (YFV) in the domain IV (26) and the SS2 loop in domain III responsible for  $\text{Na}_v1.4$  versus  $\text{Na}_v1.2$  selectivity (17). Interestingly,  $\text{Na}_v1.8$  and  $\text{Na}_v1.4$  share a homologous residue in domain III that differs from other VGSC subtypes (E1383 in  $\text{Na}_v1.8$  and E11251 in  $\text{Na}_v1.4$ ), perhaps explaining the preference of MrVIB for  $\text{Na}_v1.8$  and 1.4 over other VGSC subtypes.

The data presented here indicate that the selectivity of MrVIB for reduction in mechanical allodynia versus motor side effects is most likely because of its selectivity for  $\text{Na}_v1.8$ . This result contrasts with the poor selectivity of nonselective local anesthetics such as lignocaine. The biphasic dose–response curve that exhibits a second plateau at doses near the emergence of motor side effects is consistent with possible inhibition of other TTX-S channels at higher doses. The analgesic selectivity of MrVIB thus reflects its repertoire of VGSC-selective blockade, whereas  $\text{Na}_v1.8$  plays a major role in the excitability of nociceptors (27, 28) but is absent from larger sensory or motor neurons, allowing the selective analgesic action of MrVIB.

Antisense and gene-knockout studies have suggested different roles for  $\text{Na}_v1.8$  in neuropathic pain. Although hyperexcitability in neuromas is nearly eliminated in  $\text{Na}_v1.8$ -null mutants (12), neuropathic pain behavior appears normal (4). Compensatory up-regulation of other VGSCs may therefore contribute to the near normal phenotype. In contrast, neuropathic pain behavior

was greatly attenuated after antisense knockdown of  $\text{Na}_v1.8$  (7, 11). Furthermore, the peripheral redistribution of  $\text{Na}_v1.8$  immunoreactive material in sensory nerve endings observed in neuropathic pain states supports a role for this VGSC subtype in neuropathic pain. This study of selective analgesic actions of acute application of MrVIB in neuropathic pain further strengthens the hypothesis that  $\text{Na}_v1.8$  plays a significant role in persistent pain states. Stronger effects on mechanical pain are consistent with the known requirement for  $\text{Na}_v1.8$  in noxious mechanosensation (4). Based on these results, germ-line deletion of  $\text{Na}_v1.8$  would be expected to abolish the antinociceptive effects of low doses of MrVIB. However, such studies were not pursued because MrVIB was found to exhibit no selectivity for the TTX-R current in mouse DRG (M.D.B., unpublished results).

Although the selectivity for  $\text{Na}_v1.8$  is the most likely explanation for the MrVIB-induced analgesia without motor side effects, effects of MrVIB on other VGSC subtypes could contribute to a therapeutic effect, especially at higher concentrations of the peptide. Changes in expression (29) and spatial redistribution of other VGSCs and accessory subunits associated with neuronal damage are also likely to play a role in neuropathic pain. The absence of  $\text{Na}_v1.4$  in the CNS and the ability of MrVIB to inhibit only certain pain types after intraplantar injection argue against an involvement of  $\text{Na}_v1.4$  in the reduction in pain behavior produced by MrVIB. The analgesic effect of MrVIB is also not expected to involve inhibition of voltage-gated calcium channels, because we have demonstrated that the isotoxin MrVIA is without effect on calcium currents in rat sensory neurons (14). The presence of normal neuropathic pain in  $\text{Na}_v1.8$  or  $\text{Na}_v1.7/\text{Na}_v1.8$ -knockout mice indicates that TTX-S channels (and other channels) are able to contribute to a greater or lesser extent to altered levels of neuronal excitability (30). We propose that intrathecal MrVIB (unlike local anesthetics) selectively blocks  $\text{Na}_v1.8$  at low doses to exert a selective inhibition of noxious input in chronic pain states without effects on motor function. Taken together, these results indicate that MrVIB is a promising lead in the development of VGSC subtype-selective drugs for the treatment of chronic pain of both inflammatory and neuropathic origin, as well as potentially other pain states (31).

## Materials and Methods

**DRG Neurons.** Whole-cell  $\text{Na}^+$  currents were recorded in cultured DRG neurons isolated from 7- to 12-day-old rats by whole-cell patch clamp recording by using an Axopatch 200A patch clamp amplifier (Molecular Devices, Sunnyvale, CA). In general, neurons were cultured for 24–48 h before recording. For recording of persistent TTX-R  $\text{Na}^+$  currents ( $\text{Na}_v1.9$ ), neurons were cultured for a maximum of 24 h. Series resistance was routinely compensated by 70–80%. Capacitive and leakage currents were digitally subtracted by using a P/6 pulse protocol. Internal solution contained 10 mM NaCl, 130 mM CsF, 10 mM CsCl, 10 mM EGTA, and 10 mM Hepes–CsOH (pH 7.2), brought to 290–300 milliosmolar with sucrose. The bath solution contained 50 mM NaCl, 5 mM KCl, 5 mM  $\text{MgCl}_2$ , 1 mM  $\text{CaCl}_2$ , 10 mM glucose, 90 mM tetraethylammonium (TEA)Cl, and 10 mM Hepes-TEA-OH (pH 7.35). TTX-R  $\text{Na}^+$  currents were recorded from small DRG neurons ( $\leq 25 \mu\text{m}$  diameter) in the presence of 300 nM TTX. Large neurons ( $\geq 40 \mu\text{m}$  diameter) in which the  $\text{Na}^+$  current exhibited fast activation and inactivation kinetics and was  $>90\%$  inhibited by TTX were used to study toxin effects on TTX-S  $\text{Na}^+$  current after washout of TTX. Persistent TTX-R  $\text{Na}^+$  currents ( $\text{Na}_v1.9$ ) were recorded by using a pipette solution containing 145 mM CsCl, 3 mM  $\text{Na}_2\text{EGTA}$ , 10 mM TEACl, 10 mM Hepes, 1 mM  $\text{CaCl}_2$ , 3 mM (Mg)ATP, and 0.5 mM (Li)GTP, and a bath solution containing 43 mM NaCl, 97 mM TEACl, 10 mM Hepes, 2 mM  $\text{CaCl}_2$ , 2 mM  $\text{MgCl}_2$ , 0.5 mM

4-aminopyridine, 10 mM CsCl, 7.5 mM KCl, 0.1 mM CdCl<sub>2</sub>, and 300 nM TTX. MrVIB was dissolved in bath solution containing <0.02% DMSO and applied by a gravity-fed perfusion system.

**Xenopus Oocyte Experiments.** Capped RNA transcripts encoding full-length  $\alpha$ -subunits of rat Na<sub>v</sub>1.2 (a gift of A. Goldin, University of California, Irvine), rat Na<sub>v</sub>1.3, human Na<sub>v</sub>1.5 (a gift of R. Kass, Columbia University, New York, NY), human Na<sub>v</sub>1.7 (a gift of N. Klugbauer, Technische Universität München, Munich, Germany) and human Na<sub>v</sub>1.8 were synthesized by using a mMESSAGE mMACHINE *in vitro* transcription kit (Ambion, Austin, TX). *Xenopus laevis* stage V–VI oocytes were injected with the cRNAs encoding the VGSC subtypes (rNa<sub>v</sub>1.2; 0.5 ng per oocyte; other subtypes 2 ng per oocyte). After 3 days, whole-cell Na<sup>+</sup> channel currents were recorded by using a two-electrode (virtual ground circuit) voltage clamp at room temperature (20–23°C) with a GeneClamp 500B amplifier and pCLAMP 8 software (Axon Instruments, Union City, CA). Bath solution contained 100 mM NaCl, 2 mM KCl, 1 mM MgCl<sub>2</sub>, 0.3 mM CaCl<sub>2</sub>, and 20 mM Hepes–NaOH (pH 7.5). During recording, oocytes were perfused continuously at a rate of 1.5 ml/min. MrVIB was diluted to the appropriate concentration by direct application into the bath at maximal DMSO concentration of 0.02%. Data were low-pass filtered at 1 kHz, digitized at 10 kHz, and leak-subtracted on-line by using a –P/6 protocol and analyzed off-line. Data were analyzed by using Clampfit 8 software (Axon Instruments). Data are expressed as means ± SEM with *n* indicating the number of neurons used (*n* = 3–6). Concentration–response curves were analyzed by using Prism 3.0 (GraphPad, San Diego, CA) and fitted with a one-site binding equation,  $I_x = X_{\max}[X]^n / ([X]^n + IC_{50}^n)$ , where  $I_x$  is the inhibition by each toxin concentration,  $X$  is the toxin concentration,  $n$  is the slope factor, and  $IC_{50}$  represents the half-maximal inhibitory toxin concentration.

**<sup>125</sup>I-TxVIA Binding Assay.** We determined whether MrVIA could displace <sup>125</sup>I-TxVIA binding to VGSCs in rat brain membrane after the procedure of Fainzilber *et al.* (26).

**Intrathecal MrVIB and Local Anesthetics in Neuropathic and Inflammatory Pain.** Experiments were performed on male Sprague–Dawley rats weighing 160–300 g. Rats were housed at a maximum of six per cage. All rats were maintained on standard 12-h light/dark cycle and had free access to food and water. All behavioral groups consisted of 5 or 6 rats. Before any behavioral studies, rats were acclimatized for at least 30 min. Then, 0.15 ml of undiluted CFA (Sigma, Sydney, Australia) was injected s.c. into the plantar surface of the rear left paw. For the neuropathic pain model, rats underwent partial ligation of the left sciatic nerve (PNL) (32). Chronic polyethylene lumbar intrathecal catheters were inserted between vertebrae L5 and L6, advanced 3 cm rostrally, and exteriorized via the occipital region. All of these procedures were carried out under halothane anesthesia. Intrathecal injections were made in gently restrained animals via the exteriorized catheter, and catheter placement was confirmed by the occurrence of brief bilateral hindlimb paralysis after intrathecal lignocaine (20  $\mu$ l at 2%) after all experiments.

MrVIB and lignocaine [2-diethylamino-*N*-(2,6-dimethylphenyl)-acetamide; Sigma] were dissolved in 0.9% saline to the desired concentration on the day of the experiment and were injected in a volume of 10  $\mu$ l, followed by 15  $\mu$ l of 0.9% saline to wash the drug from the catheter dead-space. Control animals received injections of the corresponding vehicle or saline.

Mechanical PWT was measured with a series of von Frey hairs (range 0.4–15 g) by using the up-down paradigm (33). To assess thermal hyperalgesia, thermal PWL was measured by using a plantar tester (Ugo Basile, Camerio VA, Italy). To measure motor performance, ambulation was tested by using a rotarod device (Ugo Basile), with a maximal cut-off time of 300 s. All animals were acclimatized by testing mechanical PWT, thermal PWL, and rotarod latency on days 1–2. The neuropathic group underwent PNL surgery on day 3 and intrathecal catheterization on day 13, and drug effects were examined on day 17 (14 days post-PNL). The inflammatory group underwent intrathecal catheterization on day 3 and CFA injection on day 6, and drug effects were examined on day 7 (24 h post-CFA). Intrathecal catheterization had no effect on behavioral scores. MrVIB and local anesthetics were tested as described earlier.

**Intraplantar MrVIB Injections.** Rats received an initial s.c. injection of either 20  $\mu$ l (0.05  $\mu$ g/ $\mu$ l) MrVIB or 20  $\mu$ l of 0.9% saline into the plantar aspect of the left hind paw. After 5 min the rats received a s.c. injection of formalin (5%, 50  $\mu$ l). Immediately after the second injection the rats were placed in individual Plexiglas chambers. Spontaneous nociceptive behavior, biting and licking of the left hind paw, was recorded at 5-min intervals up to 1 h. In other experiments, 100  $\mu$ l (2% in 0.9% saline), 50  $\mu$ l of prostaglandin E<sub>2</sub> (100 ng in 0.9% saline), 50  $\mu$ l of carrageenan, or 50  $\mu$ l of nerve growth factor (1  $\mu$ g in 0.9% saline) was injected s.c. into the plantar surface of the left hind paw 5 min after injection of either MrVIB or saline. Effects on thermal paw withdrawal latency were determined 60, 120, 180, and 240 min after injection. All behavioral data were analyzed by using a repeated-measures analysis of variance (ANOVA), with time as a within-subjects factor, where appropriate, to compare the thresholds before and after induction of pain models and administration of drugs. Mean changes in scores produced by drug per vehicle injection were calculated as the integrated area under the time-response curve (AUC) after injection relative to levels measured 30 min before injection. When one-way ANOVAs were significant, posthoc comparisons were made against the time 0 point at 24 h post-CFA, or 14 days post-PNL (time effects), or against the vehicle-injected group, using Dunnett's adjustment for multiple comparisons. All data are presented as mean ± SEM.

**Note Added in Proof.** An article by Bulaj *et al.* (34) shows that synthetic MrVIB also has analgesic activity.

We thank Christina Schroeder and Simon Nevin for assistance with toxin isolation and oocyte testing, respectively. This work was supported by National Health and Medical Research Council (Australia) Program Grant 352446 (to R.J.L., M.J.C., and D.J.A.), National Health and Medical Research Council (Australia) Senior Principal Research Fellowship 253799 (to M.J.C.), AusIndustry (R.J.L.), the Medical Research Council (J.N.W.), and the Wellcome Trust (M.D.B.).

1. Lai J, Porreca F, Hunter JC, Gold MS (2004) *Ann Rev Pharmacol Toxicol* 44:371–397.
2. Baker MD, Wood JN (2001) *Trends Pharmacol Sci* 22:27–31.
3. Akopian AN, Sivilotti L, Wood JN (1996) *Nature* 379:257–262.
4. Akopian AN, Souslova V, England S, Okuse K, Ogata N, Ure J, Smith A, Kerr BJ, McMahon SB, Boyce S, *et al.* (1999) *Nat Neurosci* 2:541–548.
5. Djouhri L, Fang X, Okuse K, Wood JN, Berry CM, Lawson SN (2003) *J Physiol* 550:739–752.
6. Renganathan M, Cummins TR, Waxman SG (2001) *J Neurophysiol* 86:629–640.
7. Gold MS, Weinreich D, Kim CS, Wang R, Treanor J, Porreca F, Lai J (2003) *J Neurosci* 23:158–166.
8. Coggeshall RE, Tate S, Carlton SM (2004) *Neurosci Lett* 355:45–48.
9. Bucknill AT, Coward K, Plumpton C, Tate S, Bountra C, Birch R, Sandison A, Hughes SP, Anand P (2002) *Spine* 27:135–140.
10. Yiangou Y, Birch R, Sangameswaran L, Eglen R, Anand P (2000) *FEBS Lett* 467:249–252.
11. Lai J, Gold MS, Kim CS, Bian D, Ossipov MH, Hunter JC, Porreca F (2002) *Pain* 95:143–152.
12. Roza C, Laird JMA, Souslova V, Wood JN, Cervero F (2003) *J Physiol (London)* 550:921–926.
13. Lewis RJ, Garcia ML (2003) *Nat Rev Drug Discov* 2:790–802.
14. Daly NL, Ekberg JA, Thomas L, Adams DJ, Lewis RJ, Craik DJ (2004) *J Biol Chem* 279:25774–25782.

15. West PJ, Bulaj G, Yoshikami D (2005) *J Neurophysiol* 94:3916–3924.
16. Dib-Hajj SD, Tyrrell L, Black JA, Waxman SG (1998) *Proc Natl Acad Sci USA* 95:8963–8968.
17. Zorn S, Leipold E, Hansel A, Bulaj G, Olivera BM, Terlau H, Heinemann SH (2006) *FEBS Lett* 580:1360–1364.
18. Smith MT, Cabot PJ, Ross FB, Robertson AD, Lewis RJ (2002) *Pain* 96:119–127.
19. Nassar MA, Stirling LC, Forlani G, Baker MD, Matthews EA, Dickenson AH, Wood JN (2004) *Proc Natl Acad Sci USA* 101:12706–12711.
20. Khasar SG, Gold MS, Levine JD (1998) *Neurosci Lett* 256:17–20.
21. Kerr BJ, Souslova V, McMahon SB, Wood JN (2001) *NeuroReport* 12:3077–3080.
22. Okuse K, Malik-Hall M, Baker MD, Poon WY, Kong H, Chao MV, Wood JN (2002) *Nature* 417:653–656.
23. Zhang YH, Vasko MR, Nicol GD (2002) *J Physiol* 544:385–402.
24. Zhang X, Huang J, McNaughton PA (2005) *EMBO J* 24:4211–4223.
25. Fainzilber M, Kofman O, Zlotkin E, Gordon D (1995) *J Biol Chem* 270:1123–1129.
26. Leipold E, Hansel A, Olivera BM, Terlau H, Heinemann SH (2005) *FEBS Lett* 579:3881–3884.
27. Carr RW, Pianova S, Brock JA (2002) *J Gen Physiol* 120:395–405.
28. Strassman AM, Raymond SA (1999) *J Neurophysiol* 81:413–424.
29. Kim CH, Oh Y, Chung JM, Chung K (2001) *Brain Res Mol Brain Res* 95:153–161.
30. Nassar MA, Levato A, Stirling C, Wood JN (2005) *Mol Pain* 1:24.
31. Yoshimura N, Seki S, Novakovic SD, Tzoumaka E, Erickson VL, Erickson KA, Chancellor MB, de Groat WC (2001) *J Neurosci* 21:8690–8696.
32. Seltzer Z, Dubner R, Shir Y (1990) *Pain* 43:205–218.
33. Chaplan SR, Bach FW, Pogrel JW, Chung JM, Yaksh TL (1994) *J Neurosci Methods* 53:55–63.
34. Bulaj G, Zhang MM, Green BR, Fiedler B, Layer RT, Wei S, Nielsen JS, Low SJ, Klein BD, Wagstaff, JD, et al. (2006) *Biochemistry* 45:7404–7414.